ELSEVIER

Thermochimica Acta 372 (2001) 33–38

thermochimica acta

www.elsevier.com/locate/tca

Relaxation phenomena and morphology in polymer blends based on polyurethanes investigated by various thermal analysis techniques

A.S. Vatalis[a], A. Kanapitsas[b], C.G. Delides[a], P. Pissis[b,*]

[a]*Laboratories of Physics and Material Technology, Technological Education Institute (TEI) of Kozani, Kila, 50100 Kozani, Greece*

[b]*Physics Department, National Technical University of Athens, Zografou Campus, 15780 Athens, Greece*

Received 25 August 2000; accepted 8 December 2000

Abstract

The thermal, thermomechanical and thermal-dielectric properties of polyurethane blends based on branched polymer polyol (PUR) and styrene–acrylonitrile (SAN) copolymer were studied by differential scanning calorimetry (DSC), thermomechanical analysis (TMA), thermally stimulated depolarization currents (TSDC) techniques and dielectric relaxation spectroscopy (DRS). Several molecular mobility mechanisms associated with secondary local relaxations, primary (main) relaxations due to the dynamic glass transition and conductivity effects were observed and studied in detail. The use of several molecular mobility techniques, characterized by various spatial and time scales, allowed for several intercomparisons, in particular with respect to the determination of glass transition temperatures and of the temperature dependence of relaxation times which indicate the advantages and the limits of each particular technique. The results by the different techniques suggests in agreement to each other, that on addition of SAN the microphase separation between hard segment (HS) microdomains and soft segment (SS) microphase of PUR is improved.

Keywords: Polymer blends; Branched polymer polyol; Polyurethane; Styrene–acrylonitrile copolymer; Microphase separation

1. Introduction

Blending of polymers is an effective way of producing advanced multicomponent polymeric materials with new property profiles [1–3]. Segmented polyurethanes (SPUs) have often being used in multicomponent polymeric systems, such as polymer mixtures, blends and interpenetrating polymer networks [1–5], the second component being typically a thermoplastic hard polymer to improve the mechanical properties of the multicomponent system.

SPUs are characterized by microphase separation at mesoscopic length-scales into microdomains rich in hard segments (HS microdomains) and a microphase rich in soft segments (SS microphase) [6]. Specific physical and chemical interactions in SPU-based multicomponent systems may result in a modification of the degree of microphase separation (DMS) [1–7].

Here we employ differential scanning calorimetry (DSC), thermomechanical analysis (TMA), thermally stimulated depolarization currents (TSDC) techniques and dielectric relaxation spectroscopy (DRS) to study

* Corresponding author. Tel.: +30-1-7722986; fax: +30-1-7722932.
E-mail address: ppissis@central.ntua.gr (P. Pissis).

0040-6031/01/$ – see front matter
PII: S0040-6031(01)00430-0

molecular mobility, relaxation phenomena and structure–properties relationships of polyurethane blends based on branched polymer polyol (PUR) and styrene–acrylonitrile (SAN) copolymer. A main objective of this work is to investigate, by combining several techniques, and to quantify the effects of SAN on the microphase separation in PURs. Mitzner et al. [1] concluded on the basis of TMA measurements that SAN promotes microphase separation in PURs. A second main objective, from the methodological point of view, is to critically discuss, mainly on the basis of the results obtained for the glass transition temperature of PURs and the α-relaxation associated with this transition, the relationships between the various techniques employed [8].

2. Experimental

The polymer polyols were synthesized from polyoxypropylene glycol with 15 wt.% ethylene oxide termination, having an average molecular weight of 3500 and a functionality of 2.8 and styrene–acrylonitrile (SAN) copolymer with the composition 50/50 for the ratio of acrylonitrile and styrene. PUR/SAN and PUR were prepared from the polymer polyol (or polyol itself), 4,4′-diphenylmethane diisocyanate (MDI), 1,4-butandiol (BDO) in the equivalent ratio polyol/BDO/MDI = 1/1/2 (2.5% excess of MDI). The samples were prepared by the one-shot technique at 110°C and stored there for 24 h. The SAN copolymer content in the samples was 0, 10 and 20%. Details of the preparation of the samples have been given in [1].

For DSC measurements a Perkin-Elmer DSC4 differential scanning calorimeter was used (−120 to 300°C, heating rate 10°C/min). For TMA a Polymer Laboratories apparatus (Model PL-MK II) was used in shear mode in the frequency range 0.1–100 Hz from −100 to 200°C. TSDC consists of measuring the thermally activated release of frozen-in polarization and corresponds to measuring dielectric losses versus temperature at low equivalent frequencies of 10^{-4}–10^{-2} Hz [9]. The home-made equipment used has been described in [2]. Broadband dielectric relaxation spectroscopy (DRS) measurements (two-terminal complex admittance measurements) were taken using a Schlumberger frequency response analyzer (FRA 1260) supplemented by a buffer amplifier of variable gain (10^{-2}–10^{6} Hz). The temperature was controlled by a custom made nitrogen gas jet heating system covering a broad temperature range from −120 to 30°C with a resolution of ±0.02°C.

3. Results

DSC measurements provided information on the glass transition of PUR and SAN in the blends. Fig. 1 shows the specific heat increment ΔC_p at the glass transition and the glass transition temperature T_g of the SS microphase of PUR. With increasing SAN content T_g increases slightly, whereas ΔC_p decreases significantly.

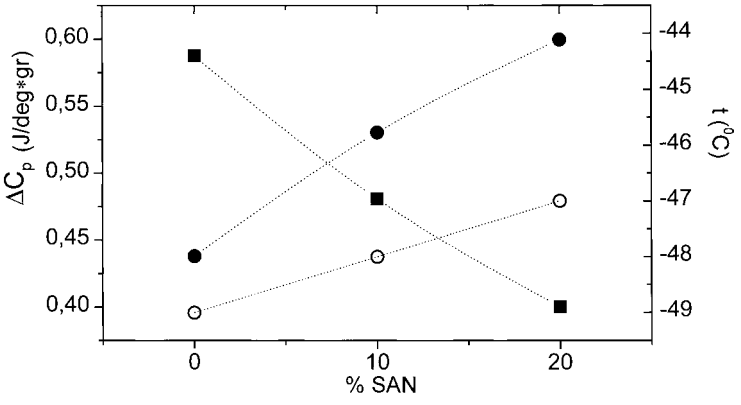

Fig. 1. Glass transition temperature (●), peak temperature of the α-relaxation in TSDC spectra (○) and specific heat increment ΔC_p (■) of the SS PUR microphase vs. SAN content.

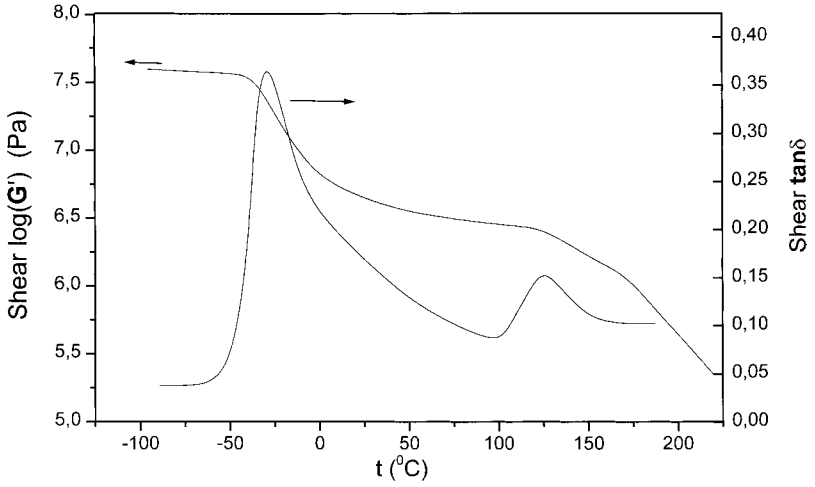

Fig. 2. TMA spectra for PUR/20% SAN at 100 Hz.

The T_g of SAN in the blends was observed for both compositions, 10 and 20% SAN, at 118°C.

Fig. 2 shows results of TMA measurements, shear modulus G' and loss tangent tan δ, for PUR/20% SAN at 100 Hz. At this frequency T_g, determined as the loss peak temperature, is −21°C for PUR and 127°C for SAN. In contrast to DSC, TMA shows a slight decrease of T_g with SAN increasing PUR content. Results obtained with the different blend compositions show an improvement of mechanical properties on addition of SAN: a plateau in G', is observed between the two T_g's, the plateau value increasing with increasing SAN content. At temperatures higher than about 180°C G' decreases significantly, in correlation with softening and melting of the HS microdomains of PUR observed by DSC.

As expected, T_g determined by TMA increases with increasing frequency of measurements. Fig. 3 shows the Arrhenius diagram for the frequency of maximum of tan δ in the temperature region of the glass transition of SAN for PUR with 20% SAN. The data are described by the following Vogel–Tammann–Fulcher–Hesse (VTFH) equation [10]:

$$f_{max} = A \exp\left(-\frac{B}{T - T_0}\right) \quad (1)$$

where A, B and T_0 (Vogel temperature) are temperature-independent empirical constants, determined as $\log A = 6.6$, $B = 212$ K and $T_0 = 366$ K. Included in the plot is the glass transition temperature T_g determined by DSC. The equivalent frequency of DSC has been obtained by the following equation [11]:

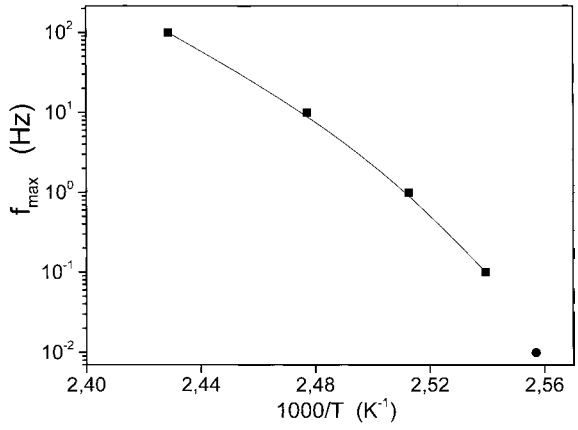

Fig. 3. Arrhenius diagram for the TMA α-relaxation in PUR/20% SAN (■). Included in the plot is the glass transition temperature T_g (●) determined by DSC.

$$f_{eq} = \frac{b}{2\pi\alpha\delta T} \quad (2)$$

where b is the cooling rate (10°C/min, equal to the heating rate), α a constant of order 1 and δT is the mean temperature fluctuation (of the order of 2°C [12]). It follows that $f_{eq} = 10$ mHz. The agreement between TMA and DSC is good.

Fig. 4 shows a typical TSDC plot measured on PUR/10% SAN. Similar plots were obtained also with

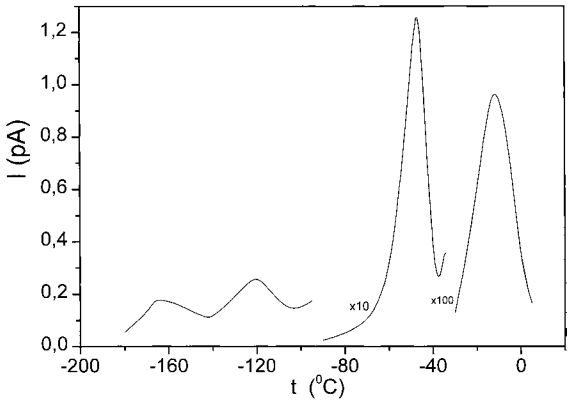

Fig. 4. TSDC spectra of PUR/10% SAN.

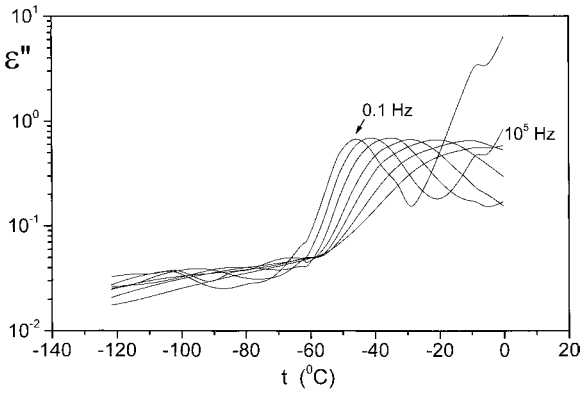

Fig. 5. Isochronal plots of dielectric losses ε'' vs. temperature for PUR/20% SAN from 0.1 to 10^5 Hz in steps of one decade.

PUR and PUR/20% SAN. Four dispersions are observed in the plots. Those at low temperatures are attributed to secondary γ- and β-relaxations in the order of increasing temperature (−160 and −120°C in Fig. 4). The peaks at high temperatures are attributed, in the order of increasing temperature, to the dipolar α-relaxation associated with the glass transition of the SS microphase and to interfacial Maxwell–Wagner–Sillars (MWS) polarization at the interfaces between HS microdomains and SS microphase [2]. For γ- and β-TSDC peaks no systematic variation of their characteristics with composition was observed. The α-peak was found to systematically shift to higher temperatures with increasing SAN content, from −49°C for PUR to −47°C for PUR/20% SAN, results for that being included in Fig. 1. The MWS peak was found to systematically shift to higher temperatures with increasing SAN content while its normalized magnitude increased, these results suggesting that DMS increases on addition of SAN [2].

Results of DRS measurements are shown in Fig. 5 for PUR/20% SAN, as isochronal plots of the

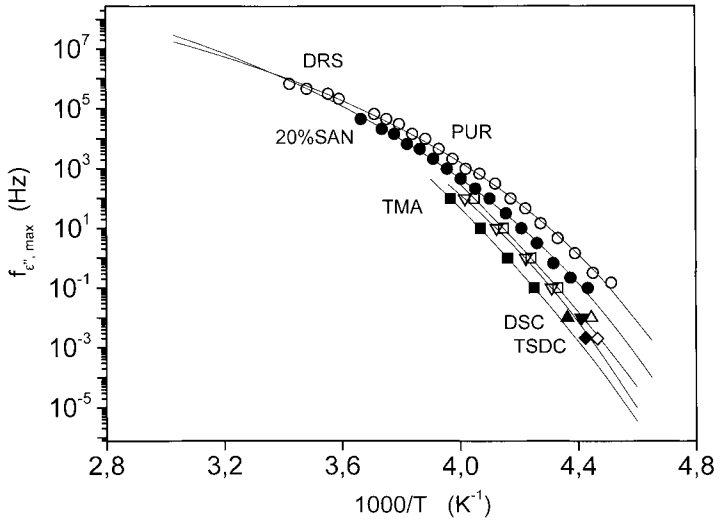

Fig. 6. Arrhenius diagram for the glass transition of SS PUR in PUR and in the blends: (○) PUR, DRS; (●) PUR/20% SAN, DRS; (□) PUR, TMA; (▽) PUR/10% SAN, TMA; (■) PUR/20% SAN, TMA; (△) PUR, DSC; (▼) PUR/10% SAN, DSC; (▲) PUR/20% SAN, DSC; (◇) PUR, TSDC; (◆) PUR/20% SAN, TSDC. The lines are VTFH fits to the data.

temperature dependence of the imaginary part of dielectric permittivity ε'' at several frequencies. The secondary β-relaxation, at lower temperatures, and the primary α-relaxation of PUR at higher temperatures, shift to higher temperatures with increasing frequency of measurements. The increase of ε'' at higher than about -30°C is due to conductivity effects [7,12].

In Fig. 6 we compare with each other, by means of the Arrhenius diagram, results obtained by different techniques for the glass transition of SS PUR in PUR and in PUR/SAN blends. In addition to DRS and TMA data, included in the plot are DSC data at the equivalent frequency of 10 mHz, Eq. (2), and TSDC data at the equivalent frequency of 1.6 mHz, corresponding to the relaxation time of 100 s [7,12]. We observe in Fig. 6 that at each temperature the α-relaxation is slightly faster in PUR as compared to PUR/20% SAN, in agreement with the TSDC and the DSC results. TMA data are shown for PUR and the two SAN samples. We observe the same trend as with the other techniques, i.e. the mechanical α-relaxation becomes slower on addition of SAN.

4. Discussion

The results by the various techniques about the effects of addition of SAN on the glass transition of SS PUR and on the corresponding a relaxation, partly summarized in Fig. 6, allow to discuss in detail and to quantify these effects. They show, in agreement with each other, that, on addition of SAN, T_g of SS PUR increases slightly (DSC, TSDC) and the associated α-relaxation becomes slightly slower (TMA, DRS). These results suggest weak interactions between SAN and SS PUR. Support for that comes from the fact that T_g of SAN does not change with PUR content (results by DSC) or decreases slightly with increasing PUR content (results by TMA).

The DSC and TSDC results provide evidence that the DMS into HS microdomains and SS microphase increases on addition of SAN, in agreement with previous TMA results [1]. For DSC, this follows from the over-proportional decrease of ΔC_p with increasing SAN content in Fig. 1, in particular for PUR/10% SAN, and increasing phase mixing, the additional contribution arising from the enhanced mobility of HS at the periphery of the HS microdomains [13]. Interestingly, a similar trend is observed for the normalized magnitude of the TSDC α-peak, which is a measure of the number of relaxing units contributing to the peak [2,9]. For TSDC, the promotion of microphase separation on addition of SAN follows from the shift of the MWS TSDC peak (Fig. 4) to higher temperatures and the increase of its magnitude with increasing SAN content. Similar systematic variations of the MWS TSDC peak in several polyurethane systems have been interpreted in terms of increasing DMS [14].

If only weak SAN–SS interactions exist, the promotion of microphase separation on addition of SAN must arise from SAN–HS interactions. Evidence for such interactions is provided by the shifting of the DSC melting endotherm attributed to softening of the HS microdomains to lower temperatures on addition of SAN, from 215°C in PUR to 210°C in PUR/20% SAN. This is in agreement with over-proportional reinforcing effects of SAN observed in the TMA experiments (this work and [1]).

With respect to intercomparison of the various techniques employed, the results in Fig. 6 for the α-relaxation in SS PUR suggest that TMA is slower than DRS, whereas DSC and TSDC are comparable to TMA. These results suggest a difference in the characteristic size of relaxing units (characteristic length scale) of DRS and TMA. Please note, however, that the complex dielectric permittivity is a compliance, whereas the complex shear modulus is a modulus, and that f_{max} in Fig. 6 refers to ε'' for DRS, whereas to $\tan\delta$ for TMA. For a more accurate comparison, transformations would be necessary [15,16]. Santagelo and Roland observed that the two techniques give different relaxation times but identical temperature dependences [17]. Diaz-Calleja et al. gave expressions to calculate the complex dielectric permittivity from mechanical results under certain conditions [18].

Both DRS and TMA work in the frequency domain and their results can be directly compared to each other at constant temperature or constant frequency, without the necessity of calculating any equivalent frequencies. In that respect, comparison of DRS and TMA results is of particular importance [8,16]. Heat capacity, shear and DRS in PVAc in the region of the

glass transition showed that in the corresponding Arrhenius diagram f_{max} increase in the order dielectric compliance, entropy compliance and shear modulus [16]. Similar measurements in polystyrene gave in the Arrhenius plot similar values for the calorimetric and dielectric data and higher values for the shear modulus data [8]. For comparison, the results for the α-relaxation of SS PUR in Fig. 6 and of SAN in Fig. 3 suggest a close correlation between TMA and DSC data.

With respect to the DRS–TSDC comparison in Fig. 6, it has been argued that the two techniques are not directly comparable, due to contribution of free charges to the TSDC α-peak [19]. However, in systems characterized by microphase-separated morphology like the PUR/SAN blends under study, free charges are expected to contribute to the MWS rather than the α-TSDC peak.

The TSDC data compare well with those of DSC in Figs. 1 and 6. This shows, in particular, that the peak temperature of the TSDC a peak is a good measure of T_g [14]. In addition, the TSDC MWS peak provides rather direct information on the microphase-separated morphology.

Acknowledgements

We would like to thank Prof. R. Becker and Dr. E. Mitzner for the preparation of samples, Dr. A. Schoenhals for using his ac equipment, and Dr. E.-H. Carrius and Dr. H. Goering for helpful discussions.

References

[1] E. Mitzner, H. Goering, R. Becker, Die Angewandte Macromolekulare Chemie 220 (1994) 177.
[2] A. Kanapitsas, P. Pissis, A. Garcia Estrella, Eur. Polym. J. 35 (1999) 923.
[3] S. Dabdin, R.P. Burford, R.P. Chaplin, Polymer 35 (1996) 923.
[4] S.P. Pandit, V.M. Nadkarni, Macromolecules 27 (1994) 4583.
[5] V. Mishra, L.H. Sperling, Polymer 36 (1995) 3593.
[6] J.T. Koberstein, A.F. Galambos, L.M. Leung, Macromolecules 25 (1992) 6195.
[7] A. Kyritsis, P. Pissis, O.P. Grigorieva, A.A. Brovko, O.N. Zimich, E.G. Privalko, V.I. Shtompel, V.P. Privalko, J. Appl. Polym. Sci. 73 (1999) 385.
[8] S. Weyer, A. Hensel, J. Korus, E. Donth, C. Shick, Thermochim. Acta 304/305 (1997) 251.
[9] J. van Turnhout, in: G.M. Sessler (Ed.), Electrets: Topics in Applied Physics, Springer, Berlin, 1980 (Chapter 3).
[10] J. Jaeckle, Rep. Prog. Phys. 49 (1986) 171.
[11] E. Donth, Relaxation and Thermodynamics in Polymers: Glass Transition, Akademie, Berlin, 1992.
[12] A. Hensel, J. Dobbertin, E.K. Schawe, A. Boller, C. Shick, Thermal Anal. 46 (1996) 935.
[13] Y.V. Savelyev, E.R. Akhranovitch, A.P. Grekov, E.G. Privalko, V.V. Korskanov, V.I. Shtompel, V.P. Privalko, P. Pissis, A. Kanapitsas, Polymer 39 (1998) 3425.
[14] A. Kanapitsas, P. Pissis, J.L. Gomez Ribelles, M. Monleon Pradas, E.G. Privalko, V.P. Privalko, J. Appl. Polym. Sci. 71 (1999) 1209.
[15] M. Tabellout, P.-Y. Baillif, H. Randrianantoandro, F. Litzinger, J.R. Emery, Phys. Rev. B 51 (1995) 12295.
[16] M. Beiner, J. Korus, H. Lockwenz, K. Schroeter, E. Dontz, Macromolecules 29 (1996) 5183.
[17] P.G. Santagelo, C.M. Roland, Macromolecules 31 (1998) 3715.
[18] R. Diaz-Calleja, E. Riande, J.S. Roman, J. Polym. Sci. Part B: Polym. Phys. 31 (1993) 711.
[19] A. Boersma, J. van Turnhout, M. Wuebbenhorst, Macromolecules 31 (1998) 7453.